MECHANIKA TEORETYCZNA
I STOSOWANA
Journal of Theoretical
and Applied Mechanics
4, 32, 1994

INFLUENCE OF STABILITY DERIVATIVES ON A QUALITY OF SIMULATION (SUPERSONIC FLOW)

TOMASZ GOETZENDORF-GRABOWSKI

Institute of Aeronautics and Applied Mechanics
Warsaw University of Technology

This work proves the influence of stability derivatives calculated with the use of computational method based on a potential model of fluid (Characteristic Box Method) on the results of numerical flight simulation. Differences between experimental and calculated results were assessed from the human receptors sensitivity thresholds point of view. The work concerns the supersonic flow.

Notations

c	–	reference chord
Cx	–	drag coefficient
Cy	–	lateral force coefficient
Cz	–	lift force coefficient
g	–	acceleration of gravity
J_x, J_y, J_z	–	moments of inertia about the body axis system
J_{xy}, J_{xz}, J_{yz}	–	products of inertia about the body axis system
J_ω	–	moment of inertia of the engine turbine
$L_P, L_R, L_{\delta v}, L_{\delta l}$	–	partial derivative of the rolling moment with respect to rolling velocity, yawing velocity, rudder deflection and ailerones deflection, respectively
$M_{\dot{w}}, M_Q, M_{\delta h}$	–	partial derivative of the pitching moment with respect to vertical acceleration, pitching velocity and elevator deflection, respectively

$N_P, N_R, N_{\delta v}$ – partial derivative of the yawing moment with respect to rolling velocity, yawing velocity and rudder deflection, respectively

m – mass of the aircraft

Ma_∞ – Mach number of the free stream flow

P – rolling velocity

Q – pitching velocity

R – yawing velocity

S – reference surface

S_x, S_y, S_z – static moments about the body axis system

T – engine thrust

V_0 – total velocity of an aircraft

u, v, w – coordinates of velocity (in the stability axis system)

x, y, z – Cartesian coordinates

X_Q – partial derivative of the aerodynamic force component along X axis with respect to the pitching velocity

$Y_P, Y_R, Y_{\delta v}$ – partial derivative of the aerodynamic force component along Y axis with respect to rolling velocity, yawing velocity and rudder deflection, respectively

$Z_Q, Z_{\delta h}$ – partial derivative of the aerodynamic force component along Z axis with respect to pitching velocity and elevator deflection, respectively

α – angle of attack

β – angle of lateral flow

$\varphi(x, y, z)$ – disturbance potential

Φ – bank angle

ϕ_{TZ}, ϕ_{TY} – angles of thrust setting

ρ – air density

Θ – pitch angle

ω – angular velocity of the engine turbine

ξ, η, ζ – Cartesian coordinates

1. Introduction

The fundamental problem in flight simulators design consists in satisfying the proper representation of real flight condition. Simulator should fly "like the aircraft". A very important element on which depends the quality of flight simulator is a mathematical model of flight dynamics. This model needs the aerodynamic characteristic of the aircraft on input. Quality of these characteristic has big influence on the quality of simulation. The aerodynamic characteristic, and stability derivatives could be obtained from experiment (eg. carried out wind tunnel or from flight test) or from calculation. Experimental investigations are very expensive and impossible to attain to in every case (eg. in the case of a quite new aircraft design). In many cases, the numerical methods for stability derivatives calculating are needed. The most often used methods for stability derivatives calculation are those basing on the potential flow model. They reveal a low cost of calculation, due to some simplifications of a flow model in comparison to the viscous one. But these simplifications could produce some errors in the results of calculations so the application of these results in the flight simulator could be impossible. This work shows the results of application of the stability derivatives obtained using the method based on the potential flow model (Prandtl-Glauert) – the Characteristic Box Method, in supersonic flow, to stability derivatives calculating for the flight simulator.

2. Physical and mathematical model of an aircraft for the flight simulation

Physical and mathematical model of an aircraft in three-dimensional motion and references systems assumed according to Maryniak (1975) are shown in Fig.1. Model was formulated on several assumptions:

- Aircraft is a rigid body with 6 degrees of freedom
- Control surfaces are movable and weightless
- Aerodynamics is stationary
- Angle of attack is small, there is no flow separation
- Atmosphere is standard, windless and not disturbed.

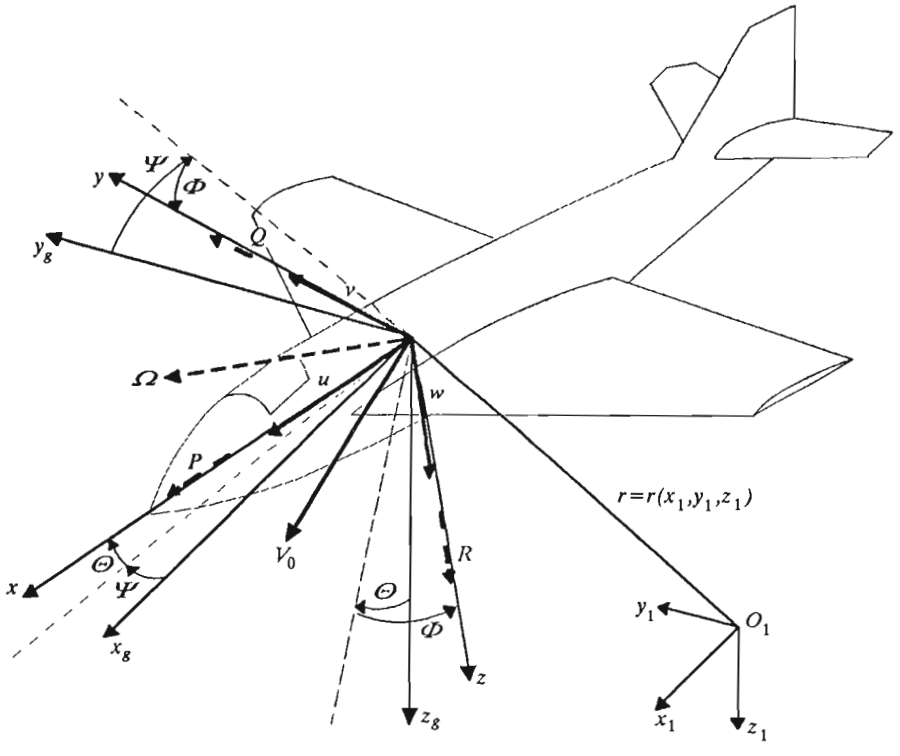

Fig. 1.

Equations of motion for the physical model defined above could be obtained using the Boltzman-Hammel equations (cf Maryniak (1975)) or employing the equations of momentum and moment of momentum balances (cf Goraj (1984)). The mathematical model is defined by six ordinary differential equations (2.1) ÷ (2.6) completed by the kinematic equations relative the assumed reference systems

$$m(\dot{u} + Qw - Rv) - S_x(Q^2 + R^2) - S_y(\dot{R} - PQ) + S_z(\dot{Q} + PR) = X \quad (2.1)$$

$$m(\dot{v} + Ru - Pw) - S_y(P^2 + R^2) + S_x(\dot{R} + PQ) - S_z(\dot{P} - QR) = Y \quad (2.2)$$

$$m(\dot{w} + Pv - Qu) - S_z(Q^2 + P^2) - S_x(\dot{Q} - PR) + S_y(\dot{P} + QR) = Z \quad (2.3)$$

$$J_x\dot{P} - (J_y - J_z)QR - J_{xy}(\dot{Q} - PR) - J_{xz}(\dot{R} + PQ) - J_{yz}(Q^2 - R^2) + \quad (2.4)$$
$$+S_y(\dot{w} - Qu + Pv) + S_z(\dot{v} - Pw + Ru) = L$$

$$J_y\dot{Q} - (J_z - J_x)RP - J_{xy}(\dot{P} - QR) - J_{yz}(\dot{R} - PQ) - J_{xz}(R^2 - P^2) + \\ -S_x(\dot{w} - Qu + Pv) + S_z(\dot{u} - Rv + Qw) = M \tag{2.5}$$

$$J_z\dot{R} - (J_x - J_y)PQ - J_{yz}(\dot{Q} + PR) - J_{xz}(\dot{P} - RQ) - J_{xy}(P^2 - Q^2) + \\ +S_x(\dot{v} - Pw + Ru) - S_y(\dot{u} - Rv + Qw) = N \tag{2.6}$$

The right-hand sides of Eqs (2.1) ÷ (2.6) represent forces and moments of forces due to aerodynamics, gravitation, engine thrust, gyroscopic effects of rolling engine elements, gear, etc. After transformation of generalised forces from the stability axis system to the body axis system, right-hand sides of Eqs (2.1) ÷ (2.6) take the form

$$X = -mg\sin\Theta + T\cos\phi_{TZ}\cos\phi_{TY} + \\ - \frac{1}{2}\rho SV_0^2(Cx_a\cos\beta\cos\alpha + Cy_a\sin\beta\cos\alpha - Cz_a\sin\alpha) + X_Q Q \tag{2.7}$$

$$Y = mg\cos\Theta\sin\Phi + T\sin\phi_{TZ} + \\ + \frac{1}{2}\rho SV_0^2(-Cx_a\sin\beta + Cy_a\cos\beta) + Y_P P + Y_R R + Y_{\delta v}\delta v \tag{2.8}$$

$$Z = mg\cos\Theta\cos\Phi - T\cos\phi_{TZ}\sin\phi_{TY} + Z_Q Q + Z_{\delta h}\delta h + \\ - \frac{1}{2}\rho SV_0^2(Cx_a\cos\beta\sin\alpha + Cy_a\sin\beta\sin\alpha + Cz_a\cos\alpha) \tag{2.9}$$

$$L = mg(y_c\cos\Theta\cos\Phi - z_c\cos\Theta\sin\Phi) - T(y_T\cos\phi_{TZ}\sin\phi_{TY} + \\ + z_T\sin\phi_{TZ}) + J_T\omega_T(R\sin\phi_{TZ} + Q\cos\phi_{TZ}\sin\phi_{TY}) + \\ + \frac{1}{2}\rho SV_0^2\left[-y_a(Cx_a\cos\beta\sin\alpha + Cy_a\sin\beta\sin\alpha + Cz_a\cos\alpha) + \right. \\ + z_a(Cx_a\sin\beta - Cy_a\cos\beta) - c(Cm_{xa}\cos\beta\cos\alpha + Cm_{ya}\sin\beta\cos\alpha + \\ \left. - Cm_{za}\sin\alpha)\right] + L_P P + L_R R + L_{\delta l}\delta l + L_{\delta v}\delta v \tag{2.10}$$

$$M = -mg(z_c \sin\Theta + x_c \cos\Theta \cos\Phi) + T(z_T \cos\phi_{TZ} \cos\phi_{TY} +$$
$$+x_T \cos\phi_{TZ} \sin\phi_{TY}) - J_T\omega_T(R \cos\phi_{TZ} \cos\phi_{TY} + P \cos\phi_{TZ} \sin\phi_{TY}) +$$
$$+\frac{1}{2}\rho S V_0^2\Big[-z_a(Cx_a \cos\beta \cos\alpha + Cy_a \sin\beta \cos\alpha - Cz_a \sin\alpha) + \qquad (2.11)$$
$$+x_a(Cx_a \cos\beta \sin\alpha + Cy_a \sin\beta \sin\alpha + Cz_a \cos\alpha) +$$
$$+c(-Cm_{xa} \sin\beta + Cm_{ya} \cos\beta)\Big] + M_{\dot w}\dot w + M_Q Q + M_{\delta h}\delta h$$

$$N = mg(x_c \cos\Theta \sin\Phi + y_c \sin\Theta) + T(x_T \sin\phi_{TZ} +$$
$$-y_T \cos\phi_{TZ} \cos\phi_{TY}) + J_T\omega_T(-P \sin\phi_{TZ} + Q \cos\phi_{TZ} \cos\phi_{TY}) +$$
$$+\frac{1}{2}\rho S V_0^2\Big[x_a(-Cx_a \sin\beta + Cy_a \cos\beta) + y_a(Cx_a \cos\beta \cos\alpha + \qquad (2.12)$$
$$+Cy_a \sin\beta \cos\alpha - Cz_a \sin\alpha) - c(Cm_{xa} \cos\beta \sin\alpha +$$
$$+Cm_{ya} \sin\beta \sin\alpha + Cm_{za} \cos\alpha)\Big] + N_P P + N_R R + N_{\delta v}\delta v$$

3. Physical and mathematical model of the flow

The physical model of flow was created on several assumptions. The most important are:

- Body of the aircraft is replaced by a thin surface (its projection on the plane according to calculating derivatives)
- Fluid is inviscid
- Flow is irrotational
- Flow is stationary
- There is a thermodynamic equilibrium.

These assumptions provide to the Prandtl-Glauert equation which determines the mathematical model of flow

$$\beta^2 \frac{\partial^2 \varphi}{\partial x^2} - \frac{\partial^2 \varphi}{\partial y^2} - \frac{\partial^2 \varphi}{\partial z^2} = 0 \tag{3.1}$$

where $\beta = \sqrt{\mathrm{Ma}_\infty^2 - 1}$ – Prandtl-Glauert coefficient.

After determining suitable boundary conditions (cf Goetzendorf-Grabowski (1994)), the solution to Eq (3.1) could be obtained in the form (cf Bertin and Smith (1989))

$$\varphi(x, y, z) = -\frac{1}{\pi} \int\int_{S(x,y,z)} \frac{w(\xi, \eta)}{R} \, d\xi d\eta \tag{3.2}$$

where

$$w = \frac{\partial \varphi}{\partial z}\Big|_{z=0} \qquad R = \sqrt{(x-\xi)^2 - \beta^2[(y-\eta)^2 + z^2]}$$

Numerical method, applied to calculation of the stability derivatives and called the Characteristic Box Method (CHB), consists of calculation first of the potential distribution from integral (3.2) and next of the pressure distribution for determined flight conditions (steady flight, flight with constant pitching velocity, etc.). Global aerodynamic characteristics could be obtained directly by integration of the pressure distribution. Details of this numerical method are given by Goetzendorf-Grabowski (1994).

4. Testing calculation

Testing calculation was done for the aircraft MiG-21. The stability derivatives, obtained from numerical calculations, were compared with the experimental data (cf Manerowski et al. (1989)) (test flight). Good agreement between them has been obtained. Relative error does not exceed 20%. The simulated calculations were done for both aerodynamic data. The results of simulation were assessed from the human receptors sensitivity thresholds point of view, so the parameters of flight, that have the considerable influence on pilot flight impression, were taken to analysis. The values of sensitivity thresholds (cf Reid and Nahon (1985)) (Tab.1) are a criterion of the simulation quality.

Table 1

threshold value for:	X	Y	Z
angular velocity [deg/s]	3.0	3.6	2.6
G-load	0.17	0.17	0.28

4.1. Computer model of simulation

A motion of the aircraft is described by an ordinary differential equation system, so the computer model of simulation could have the form (Fig.2).

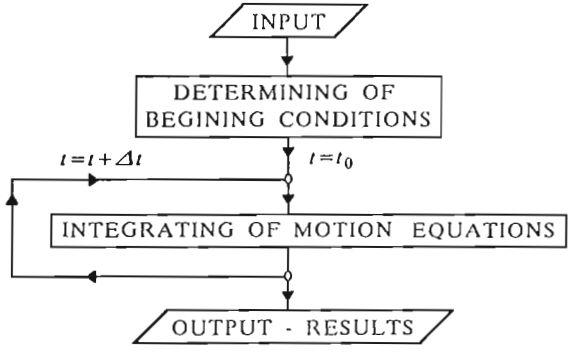

Fig. 2.

The most important part of this model, is the time loop, in which all the modules being in change of results are placed. The scheme of this part is shown in Fig.3.

Module called "AERODYNAMICS" consists of all stability derivatives obtained from two sources:

1. From experiment – "model simulation", (cf Manerowski et al. (1989))
2. From numerical calculation (CIIB).

The 4th order Runge-Kutta method modified by Merson was applied when integrating the system of differential equation of motion.

4.2. Computer model control

Fig.3 shows two different ways of control i.e. manual and automatic. Ma-

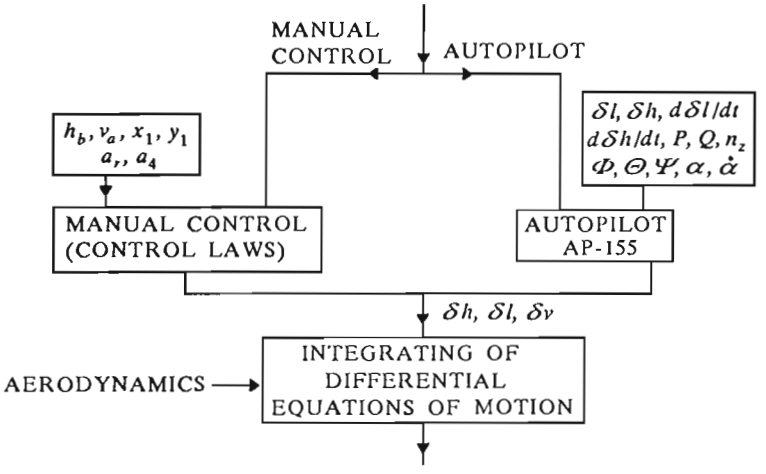

Fig. 3.

nual control is defined by a linear (cf Manerowski et al. (1989)) shift of control stick handle and rudder pedals and recalculated to control surfaces deflection, according to the following functions:

- elevator

$$\delta h = f(h_b, v_a, x_1, a_4) \tag{4.1}$$

where

δh – elevator deflection
h_b – barometric flight altitude
v_a – indicated air speed
x_1 – shift of control stick handle
a_4 – trimming tab position

- rudder

$$\delta v = A_{v_a} a_l \tag{4.2}$$

where

δv – rudder deflection
a_l – shift of the left rudder pedal
A_{v_a} – constant.

- ailerons

$$\delta l_r = A_r y_1 + B_r y_1^2 + C_r y_1^3 \tag{4.3}$$

where

δl_r – deflection of the right aileron
y_1 – shift of the control stick handle
A_r, B_r, C_r – constants.

The left aileron deflection $\delta l_l = -\delta l_r$.

The autopilot AP-155, which is placed in the MiG-21 control system, can execute different tasks. Control laws for this autopilot were determined by experiment and they are described by Manerowski et al. (1989).

4.3. Plan of testing calculation

There were five cases of testing calculation in which motion of an aircraft was simulated. Disturbances were caused by a stepwise control surfaces deflection. The motion was also tested after the autopilot was included into the system. These samples have the following beginning conditions: $1 \div 4$ – straight-line steady flight, 5 – flight with co-ordinated turn with radius 5000 m. The flight control is as follows:

1. Stepwise stick shift parallel to X-axis (elevator) ± 5 mm form the neutral stick position (conditions of equilibrium in a straight-line steady flight) (Fig.4)

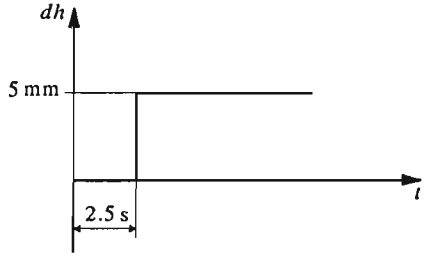

Fig. 4.

2. Stick shift parallel to X-axis -10 mm from neutral position during 2.5 s and next autopilot turn on the function "to bring into a horizontal flight" (Fig.5)

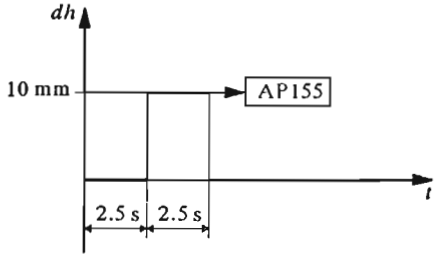

Fig. 5.

3. Stick shift parallel to Y-axis (ailerons) +10 mm from neutral position during 1 s, return to neutral position after 5 s, shift −10 mm in 1 s, and next return to neutral position (Fig.6)

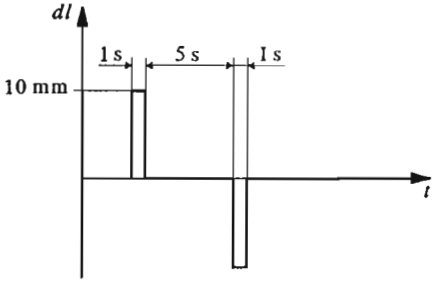

Fig. 6.

4. Rudder pedal shift in +10 mm from neutral position during 1 s, return to neutral position after 5 s, shift −10 mm for 1 s and next return to neutral position (similar to *dl* function on Fig.6)

5. Flight with co-ordinated turn at time 2.5 s, auto pilot turn on function "to bring into horizontal flight at time 5 s, and next autopilot turn on the function "to bring into beginning conditions and to stabilize the flight with them".

5. Numerical results

Calculations were done for a supersonic flow, for airspeeds defined by the following Mach numbers: 1.2, 1.4, 1.6, 1.8. Two of them (Ma = 1.2, 1.6)

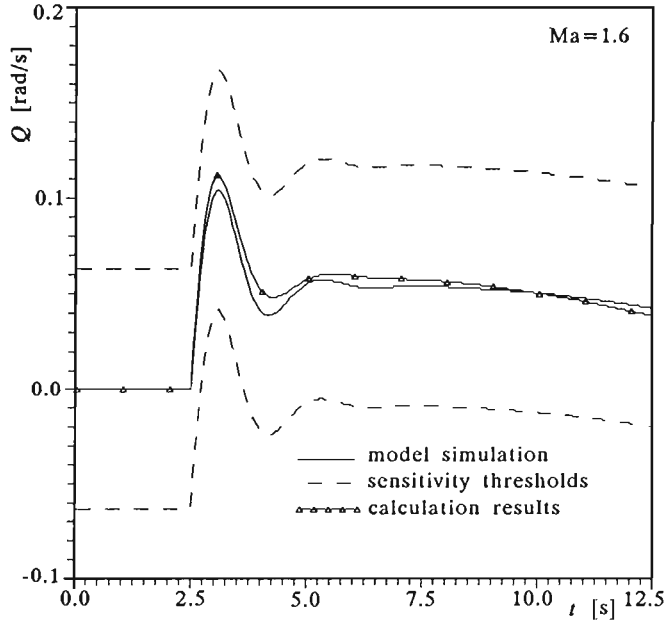

Fig. 7. Pitching angular velocity Q due to the negative stepwise elevator deflection

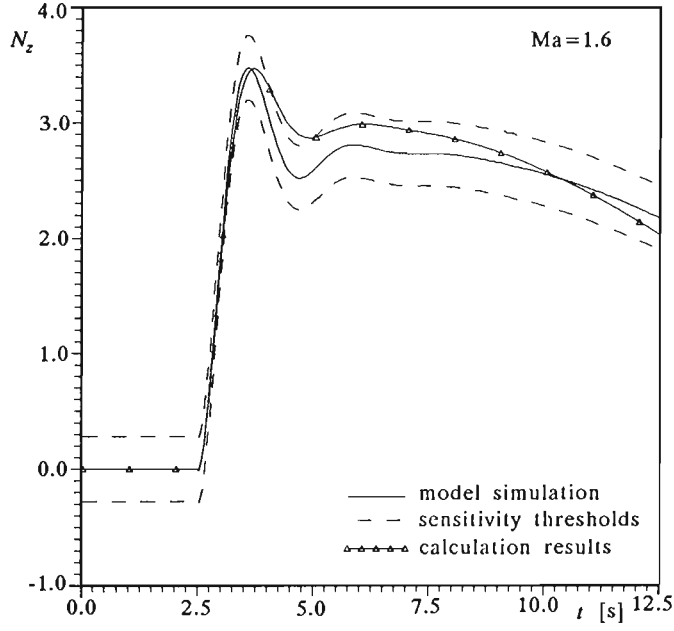

Fig. 8. G-load coefficient parallel to Z axis due to the negative stepwise elevator deflection

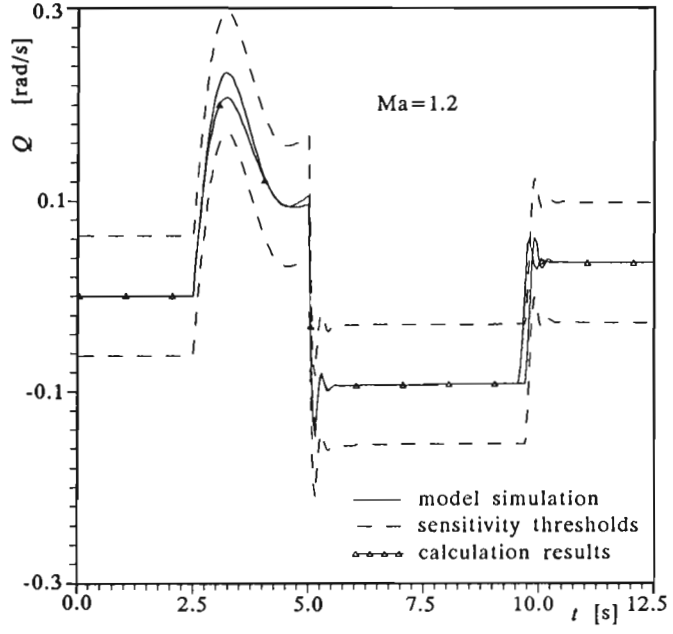

Fig. 9. Pitching angular velocity Q due to the negative stepwise elevator deflection and after autopilot was included into the system

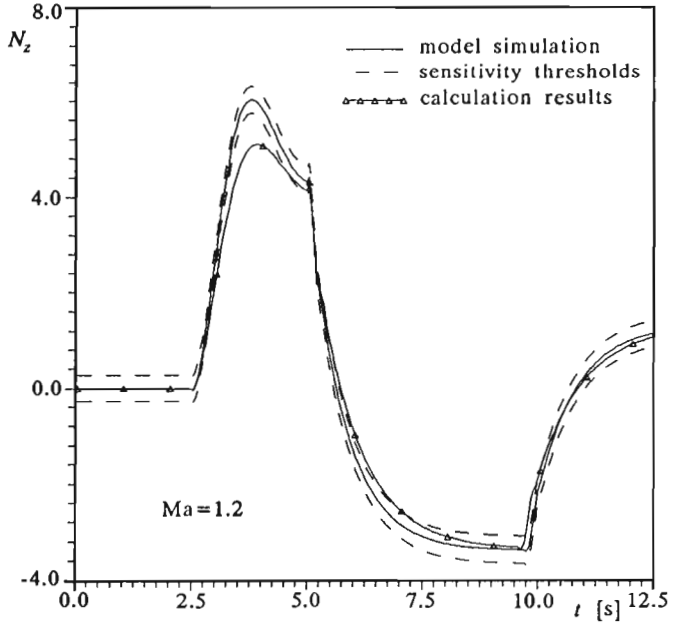

Fig. 10. G-load coefficient parallel to Z axis due to the negative stepwise elevator deflection and after autopilot was included into the system

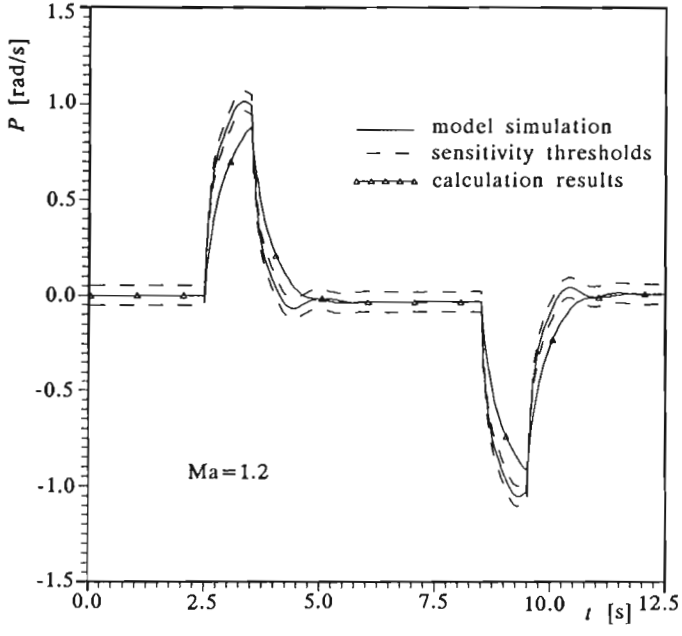

Fig. 11. Rolling angular velocity P due to the stepwise ailerones deflection

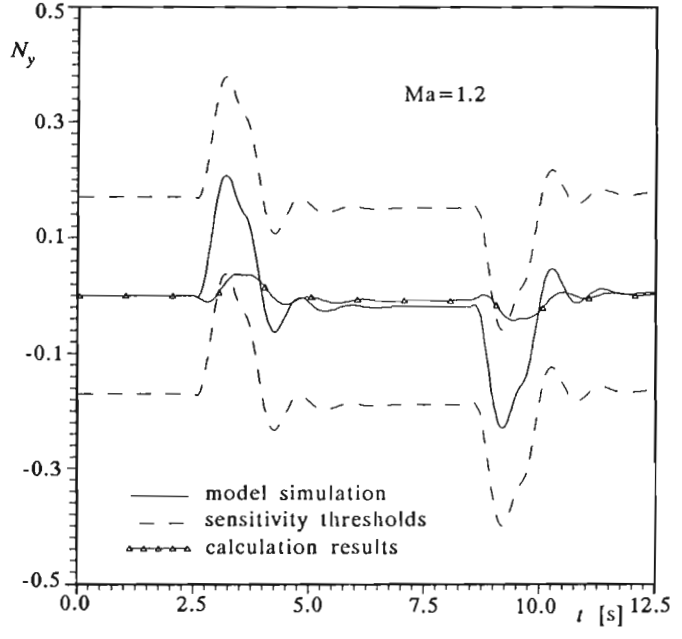

Fig. 12. G-load parallel to Y axis due to the stepwise ailerones deflection

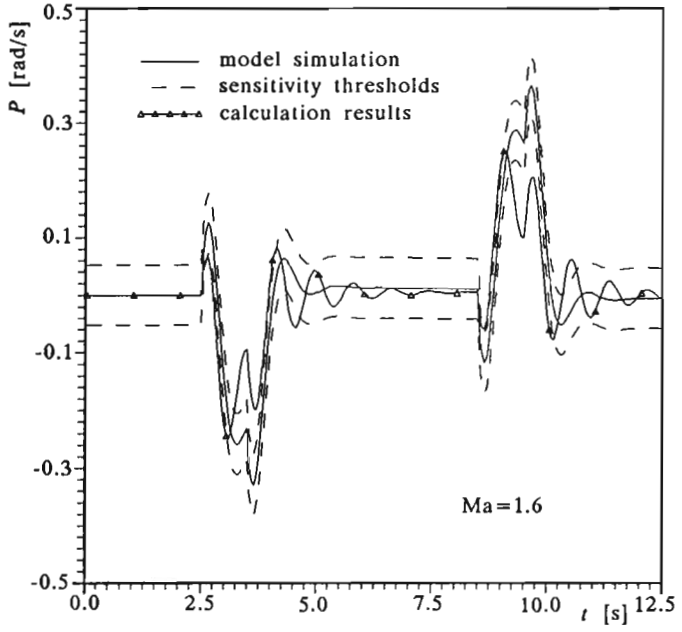

Fig. 13. Rolling angular velocity P due to the stepwise rudder deflection

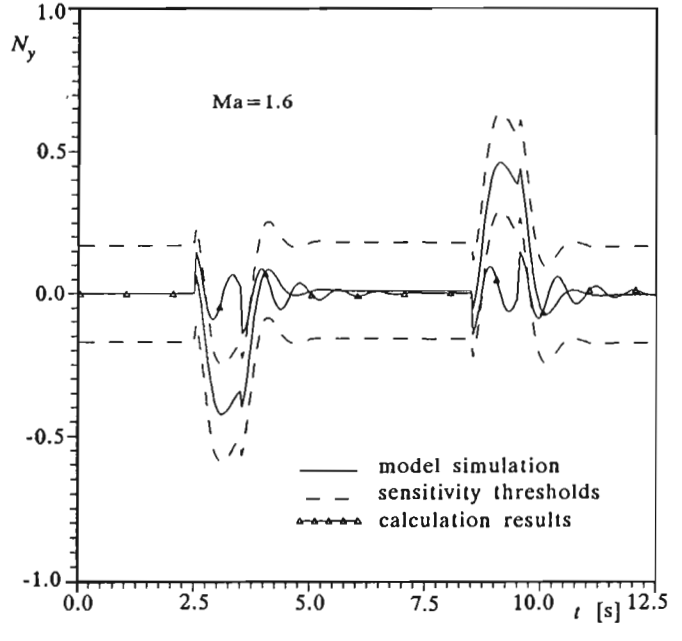

Fig. 14. G-load parallel to Y axis due to the stepwise rudder deflection

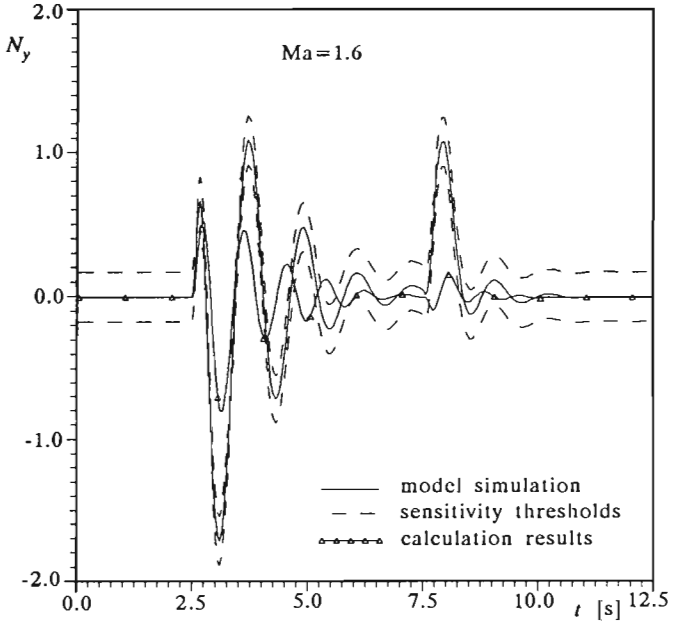

Fig. 15. G-load parallel to Y axis in turn with radius $R = 5000$ m

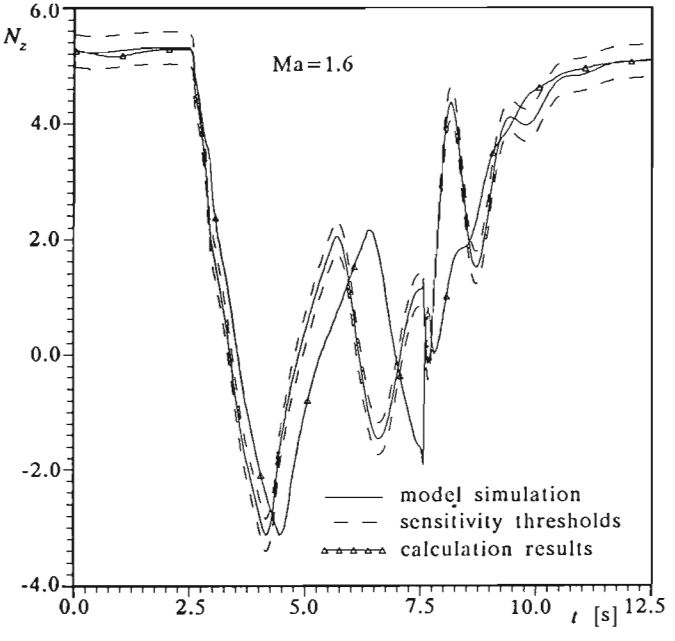

Fig. 16. G-load parallel to Z axis in turn with radius $R = 5000$ m

were taken to a presentation, due to the most representative results obtained for these samples.

Figures 7 and 8 present the simulation results for the 1th case of control function – stepwise stick movement in the elevator channel. Fig.7 shows pitching angular velocity Q due to the control function from Fig.4, and Fig.8 present the G-load parallel to the Z axis due to the same control function. The results of simulation with the control function shown in Fig.5 – stepwise stick moving in elevator channel and next controlled by autopilot, are presented by the same variables as in the previous case (Q and N_z) and are shown in the Fig.9 and Fig.10. Figures 11 and 12 present the results of simulation for the 3rd case of control function (Fig.6) – stepwise stick movement in the ailerons channel. The rolling angular velocity P due to this control function is shown in Fig.11 and the G-load parallel to Y-axis N_y in Fig.12. Figures 13 and 14 present the same variables as the previous ones but for the 4th case of control function – stepwise rudder pedal movement (function similar to the stick movement in Fig.6). The simulation results of flight with co-ordinated turn – case No.5, are presented in Fig.15 and Fig.17. First of them shows the G-load parallel to Y-axis N_y and the second one the G-load parallel to Z-axis N_z. Fig.17 presents the rolling angular velocity P.

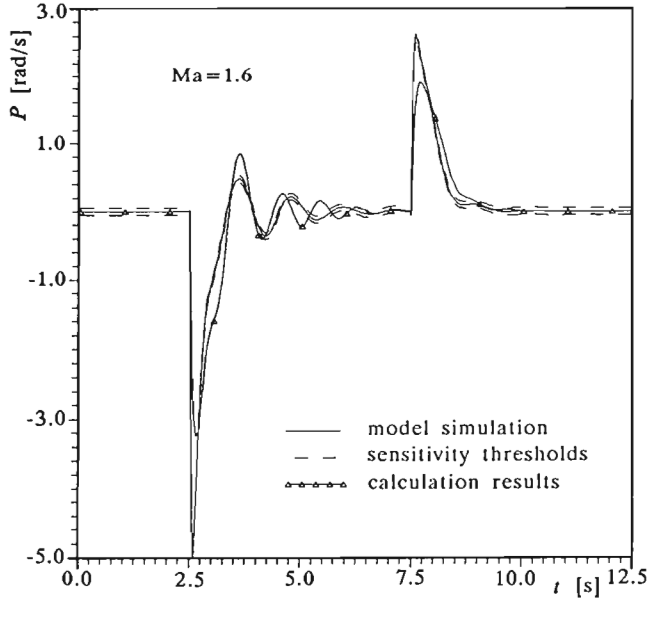

Fig. 17. Rolling angular velocity in turn with radius $R = 5000$ m

All the results of simulation are compared with the results of "model simulation" – simulation with aerodynamic data (stability derivatives) from test flight. Dashed lines in these figures denote the sensitivity threshold values of human receptors, so if the curve denoted "calculating results" is placed between them, then the differences are not noticed by the pilot, and the quality of simulation could be regarded as good. However, "calculating results" exceed the interval created by sensitivity thresholds, the differences are not big.

6. Concluding remarks

From the results obtained from calculations we can state, that the test of application of stability derivatives, obtained from presented method, to the flight simulation, was successful. Scatter (from "model simulation") of results was bigger in the cases, where lateral derivatives were the decisive ones. It is caused by modelling even wide bodies with the air of thin surfaces. We can suppose, that if we considered the thickness of wide elements of an aircraft (fuselage, nacelle etc.), the results would be improved. Then, stability derivatives obtained by means of the presented numerical method could be applied to flight simulators.

References

1. BERTIN J.J., SMITH M.L., 1989, *Aerodynamics for Engineers,* Prentice-Hall International, Inc., London

2. GOETZENDORF-GRABOWSKI T., 1994, Numerical Calculation of Stability Derivatives of an Aircraft, *Journal of Theoretical and Applied Mechanics,* **32**, 3

3. GORAJ Z., 1984, Obliczenia sterowności równowagi i stateczności samolotu w zakresie poddźwiękowym, *Wyd. Politechniki Warszawskiej,* Warszawa

4. MANEROWSKI J., NOWAKOWSKI M., KOCZOROWSKI Z., KRUTKOW A., RYMASZEWSKI S., ZAGDANSKI Z., ZGRZYWA F., 1989, Opracowanie modelu samolotu MiG-21BIS, Warszawa (unpublished)

5. MARYNIAK J., 1975, Dynamiczna teoria obiektów ruchomych, *Prace Naukowe Politechniki Warszawskiej, Seria Mechanika,* 32, Warszawa

6. REID L.D., NAHON M.A., 1985, Flight Simulation Motion-Base Drive Algorithms, Part 1 – Developing and Testing the Equations, *UTIAS Report,* No.296

Wpływ pochodnych aerodynamicznych na jakość symulacji (zakres naddźwiękowy)

Streszczenie

W pracy pokazano wpływ charkterystyk aerodynamicznych samolotu, otrzymanych przy użyciu metody obliczeniowej bazującej na potencjalnym modelu opływu (Metoda Siatki Rombowej) na wyniki symulacji numerycznej lotu. Różnice między wynikami obliczeń i rezultatami doświadczalnymi oceniono pod kątem czułości progowej odpowiednich receptorów człowieka.

Manuscript received February 7, 1994; accepted for print May 24, 1994